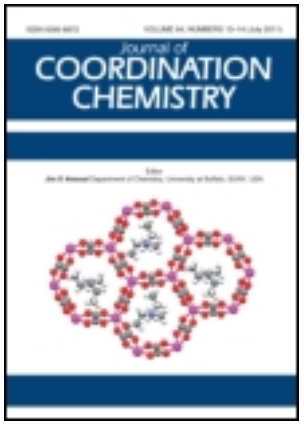

Journal of Coordination Chemistry
Publication details, including instructions for authors and subscription information:
http://www.tandfonline.com/loi/gcoo20

Introducing p-block metals into iodoargentates: structures and properties of two new heterometallic hybrids

Haohong Li [a b], Junbo Li [a], Min Wang [a], Shuwei Huang [a], Anweng Gong [a], Hongyang Wu [a] & Zhirong Chen [a b]

[a] College of Chemistry and Chemical Engineering, Fuzhou University, Fuzhou, Fujian 350108, China

[b] State Key Laboratory Breeding Base of Photocatalysis, Fuzhou University, Fuzhou 350002, China

Accepted author version posted online: 10 Sep 2012.Published online: 21 Sep 2012.

To cite this article: Haohong Li, Junbo Li, Min Wang, Shuwei Huang, Anweng Gong, Hongyang Wu & Zhirong Chen (2012) Introducing p-block metals into iodoargentates: structures and properties of two new heterometallic hybrids, Journal of Coordination Chemistry, 65:21, 3851-3859, DOI: 10.1080/00958972.2012.727405

To link to this article: http://dx.doi.org/10.1080/00958972.2012.727405

Journal of Coordination Chemistry
Vol. 65, No. 21, 10 November 2012, 3851–3859

Introducing p-block metals into iodoargentates: structures and properties of two new heterometallic hybrids

HAOHONG LI*†‡, JUNBO LI†, MIN WANG†, SHUWEI HUANG†, ANWENG GONG†, HONGYANG WU† and ZHIRONG CHEN*†‡

†College of Chemistry and Chemical Engineering, Fuzhou University, Fuzhou, Fujian 350108, China
‡State Key Laboratory Breeding Base of Photocatalysis, Fuzhou University, Fuzhou 350002, China

(*Received 21 November 2011; in final form 10 August 2012*)

Two new heterometallic complexes, $[Bi(phen)I_4Ag(phen)]_n$ (**1**) and $[Pb(bipy)Ag_3I_5]_n$ (**2**) (phen = 1,10-phenanthroline, bipy = 2,2′-bipyridine), have been synthesized, significant for incorporation of heavy p-block metals (Pb and Bi) into iodoargentate frameworks to get heterometallic complexes. Complex **1** could be described as the combination of $Ag(phen)I_4$ and $Bi(phen)I_4$ octahedra by edge-sharing and **2** is constructed from $(Ag_3I_5)_n^{2n-}$ and $[Pb(2,2'\text{-bipy})]^{2+}$ by Pb–I covalent bonds. Their optical band gaps, fluorescences, and thermal behaviors are also discussed.

Keywords: Heterometallic iodoargentate; Hybrid semiconductor; Optical adsorption

1. Introduction

Syntheses of hybrid materials through modification of metal halides by ligands have significance for opt-electronic materials, nonlinear optical materials, luminescence thermochroism materials, and visible-light sensitizers for photovoltaic cells [1–6]. For silver halide systems, incorporation of organic components into silver/halide structures has been realized by using low-temperature procedures [7–12]. A recent advance in this system is obtaining materials by introducing a heterometal together with ligands into silver halide inorganic skeletons [13–18]. Two situations have been found: (1) the second metal coordinates with ligands (ML_n) to act as structure directing agent without direct binding with the inorganic frameworks and (2) the second metal dopes into the silver halide skeleton to give heterometallic frameworks. In the former case, progress has been made with some transition metals (Ni^{2+}, Cu^{2+}, Zn^{2+}, etc.) [17, 18] and lanthanide metals (Tb^{3+}, Y^{3+}) [13, 14] introduced. For the latter case, much less work, especially incorporating heavy main group metal, has been done [17]. Pb(II) and Bi(III) exhibit a variety of coordination numbers and stereochemical activities with or without the effect of the lone pair of electrons in the coordination sphere. We focus our attention on

*Corresponding authors. Email: lihh@fzu.edu.cn; zrchen@fzu.edu.cn

ISSN 0095-8972 print/ISSN 1029-0389 online
http://dx.doi.org/10.1080/00958972.2012.727405

metals with a $6s^2$ lone pair to modify the micro-structure and properties of iodoargentates. Herein, we incorporate Pb and Bi into iodoargentate frameworks to get heterometallic complexes, and two new heterometallic (Bi/Pb) iodoargentate hybrids and their properties are discussed.

2. Experimental

2.1. *Materials and methods*

All chemicals were of reagent grade quality obtained from commercial sources and used without purification. Elemental analyses for C, H, and N were performed on a Vario MICRO elemental analyzer. IR spectra were recorded on a Perkin-Elmer Spectrum-2000 FTIR spectrophotometer (4000–400 cm^{-1}) on powdered sample spread on a KBr plate. Optical diffuse reflectance spectra were measured on a Perkin-Elmer lambda 900 UV/Vis spectrophotometer equipped with an integrating sphere at 293 K, and a $BaSO_4$ plate was used as reference. Photoluminescence measurements were carried out on an Edinburgh ELS920 fluorescence spectrometer. X-ray powder diffractions were performed on an X-ray MiniFlexII diffractometer. Thermal analyses were performed under nitrogen with a heating rate of 10°C min^{-1} on a NETZSCH TG209 F3 instrument.

2.2. *Synthesis of [Bi(phen)I_4Ag(phen)]$_n$ (1)*

A DMF solution (15 mL) containing 0.408 g $AgNO_3$ (2.4 mmol), $Bi(NO_3)_3 \cdot 5H_2O$ (0.581 g, 1.2 mmol), and 0.360 g NaI (2.4 mmol) was stirred for 1 h at 50°C. Afterwards, 0.408 g phenanthroline (1.2 mmol) was added into the above solution and kept for 3 h with continuous stirring. The pH of resultant solution was adjusted to 4.5 by 57% HI. The hot solution was filtered and the filtrate was kept for five days at room temperature. Red block crystals were obtained in 58% yield based on phen. Elemental Anal. Calcd (%) for $C_{24}H_{16}AgBiI_4N_4$: C, 24.31; H, 1.35; N, 4.73. Found (%): C, 24.38; H, 1.31; N, 4.67. IR (KBr, cm^{-1}): 3437(m), 3043(w), 1619(w), 1587(w), 1514(s), 1494(m), 1423(s), 1343(m), 1219(w), 1141(m), 1098(m), 861(w), 843(s), 775(w), 721(s), 639(w), 470(w), 416(w). UV-Vis: 220, 259, 403, 466 nm (Supplementary material).

2.3. *Synthesis of [Pb(bipy)Ag_3I_5]$_n$ (2)*

A DMF solution (15 mL) containing 0.553 g PbI_2 (1.2 mmol) and $AgNO_3$ (0.408 g, 2.4 mmol) was stirred for 1 h at 50°C. Then 0.187 g 2,2′-bipyridine (1.2 mmol) was added. The reaction was kept for an additional 3 h with continuous stirring and the pH was adjusted to 4.5 by adding 57% HI. The solution was filtered and the pale-yellow filtrate was kept for three days at room temperature. Yellow block crystals were obtained in 63% yield based on Ag. Elemental Anal. Calcd (%) for $C_{10}H_8Ag_3I_5N_2Pb$: C, 9.09; H, 0.61; N, 2.12. Found (%): C, 9.05; H, 0.58; N, 2.17. IR (KBr, cm^{-1}): 3448(m), 3020(w), 1851(w), 1590(s), 1568(m), 1491(m), 1471(m), 1434(s), 1310(m),

1242(m), 1208(w), 1172(w), 1154(m), 1102(m), 1063(w), 1012(s), 769(s), 726(w), 648(m), 629(m), 473(w), 408(w). UV-Vis: 250, 314, 386 nm (Supplementary material).

2.4. *X-ray crystallography*

The intensity data of **1** and **2** were collected on a Rigaku Weissenberg IP diffractometer using graphite-monochromated Mo-Kα radiation ($\lambda = 0.71069$ Å) at 293(2) K. Corrections of *Lp* factors and multi-scan absorption were applied. The structures were solved by direct methods and refined on F^2 by full-matrix least squares using SHELXTL-97 [19]. All non-hydrogen atoms were refined anisotropically. Hydrogen atoms (C–H) were generated geometrically. Crystallographic data and refinement details of **1** and **2** are listed in table 1. Selected bond lengths and angles are given in tables 2 and 3, respectively; π–π stacking interactions and hydrogen-bond data are listed in tables 4 and 5.

Table 1. Crystallographic data and refinement parameters for **1** and **2**.

Complex	**1**	**2**
Empirical formula	$C_{24}H_{16}AgBiI_4N_4$	$C_{10}H_8Ag_3I_5N_2Pb$
Formula weight	1184.86	1321.49
Crystal system	Monoclinic	Monoclinic
Space group	*C*2	*Cc*
Unit cell dimensions (Å, °)		
a	16.678(9)	11.296(5)
b	11.236(7)	22.570(15)
c	7.815(4)	8.089(4)
β	105.58(2)	92.720(16)
Volume (Å^3), *Z*	1410.7(14), 2	2060.0(19), 4
Calculated density (g cm^{-3})	2.789	4.261
Absorption coefficient (mm^{-1})	11.320	18.445
F(000)	1060	2280
Reflections, total	6972	10,079
Reflections, unique	3164 ($R_{int} = 0.0412$)	4169 ($R_{int} = 0.0446$)
Reflections, observed	2932	3914
Goodness-of-fit on F^2	1.065	1.113
No. of parameters refined	84	199
R_1 [$I > 2\sigma(I)$]	0.0413	0.0356
wR_2 [$I > 2\sigma(I)$]	0.0997	0.1033
Residual extremes (e Å^{-3})	1.512 and −1.102	1.559 and −1.203

Table 2. Selected bond lengths (Å) and angles (°) for **1**.

Bi(1)–N(1)	2.510(12)	Bi(1)–N(1)#1	2.510(12)
Bi(1)–I(1)#1	3.0149(14)	Bi(1)–I(1)	3.0149(14)
Bi(1)–I(2)#1	3.0667(14)	Bi(1)–I(2)	3.0667(14)
Ag(1)–N(2)	2.403(14)	Ag(1)–N(2)#2	2.403(14)
Ag(1)–I(2)	2.9653(18)	Ag(1)–I(2)#2	2.9653(18)
Ag(1)–I(1)	3.289(25)	Ag(1)–I(1) #2	3.289(25)
I(1)#1–Bi(1)–I(2)#1	94.18(4)	I(1)–Bi(1)–I(2)#1	91.95(4)
I(1)#1–Bi(1)–I(2)	91.95(4)	I(1)–Bi(1)–I(2)	94.18(4)
I(2)#1–Bi(1)–I(2)	169.92(4)		

Symmetry codes: #1: $-x+1, y, -z$; #2: $-x+1, y, -z+1$.

Table 3. Selected bond lengths (Å) and angles (°) for **2**.

Pb(1)–N(1)	2.446(14)	Pb(1)–N(2)	2.458(12)
Pb(1)–I(1)	3.080(24)	Pb(1)–I(5)#1	3.365(27)
Pb(1)–I(4)	3.453(20)	Ag(1B)– I(1)	2.781(4)
Ag(1B)–I(2)	2.814(14)	Ag(1B)–I(3)	2.832(13)
Ag(1B)–I(3)#2	2.975(19)	Ag(2)–I(4)	2.868(7)
Ag(2)–I(3)	2.8163(19)	Ag(2)–I(5)	2.871(2)
Ag(2)–I(4)#1	2.802(13)	Ag(3)–I(4)	2.956(2)
Ag(3)–I(5)	2.785(2)	Ag(3)–I(2)#5	2.82(2)
Ag(3)–I(2)#6	2.859(20)	Ag(3)–Ag(2)	3.266(18)
I(1)–Pb(1)–I(5)#1	165.56(3)	Ag(1B)–I(2)–Ag(3)#3	112.95(6)
Ag(1B)–I(2)–Ag(3)#4	127.72(6)	Ag(2)–I(4)–Ag(3)	68.19(5)
Ag(2)#2–I(4)–Ag(2)	109.41(5)	Ag(2)#2–I(4)–Ag(3)	100.33(5)
Ag(3)#3–I(2)–Ag(3)#4	101.16(6)	Ag(3)–I(5)–Ag(2)	70.51(5)
Ag(3)#4–I(2)–Ag(1)#2	86.5(2)	I(2)#6–Ag(3)–Ag(2)	107.62(5)
I(2)#5–Ag(3)–I(2)#6	91.57(5)	I(2)#5–Ag(3)–I(4)	107.23(5)
I(2)#6–Ag(3)–I(4)	99.81(5)	I(2)#5–Ag(3)–Ag(2)	154.94(6)
I(3)–Ag(2)–I(4)	100.97(5)	I(3)–Ag(2)–I(5)	114.58(5)
I(4)–Ag(3)–Ag(2)	54.63(4)	I(4)#1–Ag(2)–I(3)	120.13(5)
I(4)#1–Ag(2)–I(4)	113.65(5)	I(4)#1–Ag(2)–I(5)	102.70(5)
I(4)–Ag(2)–I(5)	104.08(5)	I(4)#1–Ag(2)–Ag(3)	97.85(5)
I(5)–Ag(3)–I(2)#5	123.83(6)	I(5)–Ag(3)–I(2)#6	127.27(6)
I(5)–Ag(3)–I(4)	103.99(6)	I(5)–Ag(3)–Ag(2)	55.97(4)

Symmetry codes: #1: $x, -y+1, z+1/2$; #2: $x, -y+1, z-1/2$; #3: $x-1, y, z$; #4: $x-1, -y+1, z-1/2$; #5: $x+1, y, z$; #6: $x+1, -y+1, z+1/2$.

Table 4. $\pi-\pi$ Stacking interactions for **1**.

Cg(I)···Cg(J)	Symmetry code	Centroid distance (Å)	Dihedral angle (°)	CgI_Perp distance (Å)	CgJ_Perp distance (Å)
Cg(1) → Cg(4)	$x, 1+y, z$	3.813(10)	2.3(8)	3.356(6)	3.425(6)
Cg(2) → Cg(3)	$x, -1+y, z$	3.816(10)	3.7(7)	3.312(7)	3.408(6)

Ring Cg(1): N(1) → C(1) → C(2) → C(3) → C(4) → C(5) →
Ring Cg(2): N(2) → C(7) → C(8) → C(9) → C(10) → C(11) →
Ring Cg(3): C(4) → C(5) → C(5)a → C(4)a → C(6)a → C(6) →
Ring Cg(4): C(10) → C(11) → C(11)b → C(10)b → C(12)b → C(12) →

Table 5. Intramolecular hydrogen-bond lengths (Å) and angles (°) for **2**.

D–H···A	*d*(D–H)	*d*(H···A)	*d*(D···A)	∠DHA
C(1)–H(1)···I(3)#1	0.93	3.01	3.845(16)	149.65
C(10)–H(10)···I(4)	0.93	2.98	3.778(16)	144.96

Symmetry codes: #1: $x, 1-y, 1/2+z$.

3. Results and discussion

3.1. *Crystal structures*

The structure of **1** could be described as the combination of $Ag(phen)I_4$ and $Bi(phen)I_4$ octahedra by edge-sharing to give an infinite chain along the *c*-axis (figure 1). In the distorted AgI_4N_2 octahedron, Ag–I bonds are non-uniform, ranging from 2.9653(18) to 3.289(25) Å with an average (av) of 3.1271 Å, longer than those of other silver iodide bonds, e.g., $[Ag_2I_4]_n^{2n-}$ in $[Zn(en)_3(Ag_2I_4)]_n$, whose Ag–I distances range from 2.8529(10)

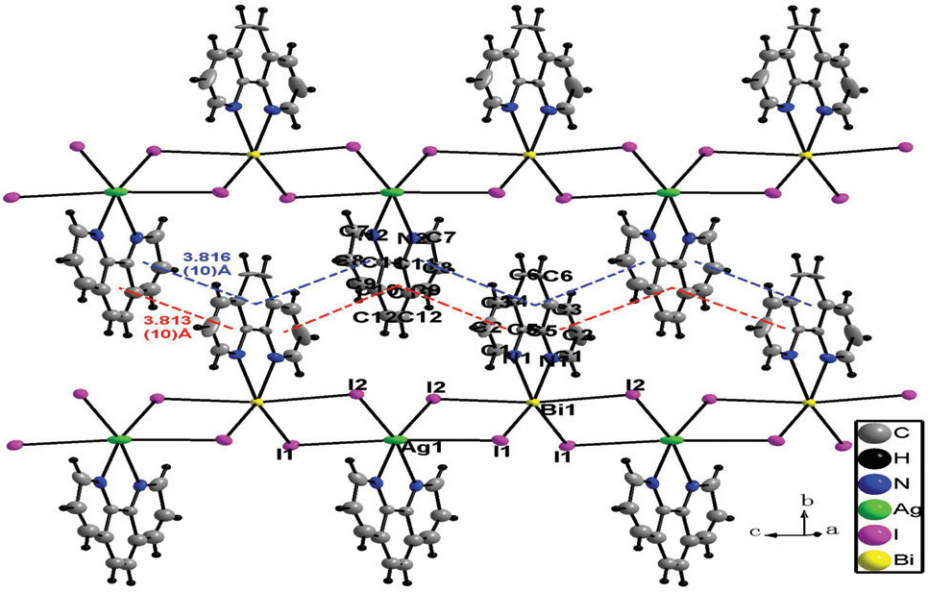

Figure 1. 2-D layer based on π–π stacking interactions (red and blue dashed lines) between phen rings belonging to adjacent 1-D chains.

to 2.890(3) Å [15]. In the BiI_4N_2 octahedron, Bi–I bonds range from 3.0149(14) to 3.0667(14) Å, which are comparable to $Bi–I_{bridging}$ bond lengths (2.9370(14)–3.0205(12) Å) in $\{[MQ]_3[Bi_2I_6(\mu\text{-}I)_3][Bi_2I_6(\mu\text{-}I)_2(MQ)_2]_3$ [20]. All Ag–N and Bi–N distances are in the normal range. The Bi–Ag distance is 4.262(2) Å, illustrating the absence of metal–metal interaction. All phen rings are parallel and centroid distances of adjacent phen rings at the same side of the chain are 7.815 Å, indicating the absence of direct π–π stacking interactions. However, strong π–π stacking interactions exist between phen rings belonging to adjacent 1-D chains with centroid distances of 3.813(10) and 3.816(10) Å (table 4), so the 1-D chains of **1** extend into a 2-D layer along the *bc*-plane (figure 1).

We describe the crystal structure of **2** as the combination of $[Pb(2,2'\text{-bipy})]^{2n+}$ and $(Ag_3I_5)_n^{2n-}$ by Pb–I covalent bonds. As shown in figure 2(a), the structure of $(Ag_3I_5)_n^{2n-}$ framework could be depicted as Ag_6I_{14} building blocks, in which each silver has an I_4 donor set and pseudo-tetrahedral geometry. Ag_6I_{14} building blocks can be divided into two Ag_3I_7 sub-units. In the Ag_3I_7 sub-unit, $Ag(1)I_4$ tetrahedra connect with $Ag(2)I_4$ tetrahedra *via* vertex-sharing [Ag(1) is disordered with occupancy of 15% (Ag1A) and 85% (Ag1B); we here only discuss Ag(1B)], but $Ag(2)I_4$ tetrahedra bind with $Ag(3)I_4$ tetrahedra *via* edge-sharing. Here, the $Ag(1)I_4$ tetrahedron is distorted with Ag–I distances in the range of 2.714(10)–3.135(26) Å, and $Ag(2)I_4$, $Ag(3)I_4$ tetrahedra are in the normal range. Due to edge-sharing, strong Ag···Ag interaction [Ag(2)–Ag(3)] could be found with Ag···Ag distance of 3.266(18) Å. The attraction between d^{10}–d^{10} closed-shell metals promotes the aggregation of silver(I) centers, supported by spectroscopic and structural evidence [21]. Two Ag_3I_7 sub-units give the Ag_6I_{14} building block by *c* gliding face symmetry operation. Extending of $(Ag_3I_5)_n^{2n-}$ framework is completed in two directions (*a* and *c*); along the *c*-axis, Ag_6I_{14} building blocks extend to an infinite

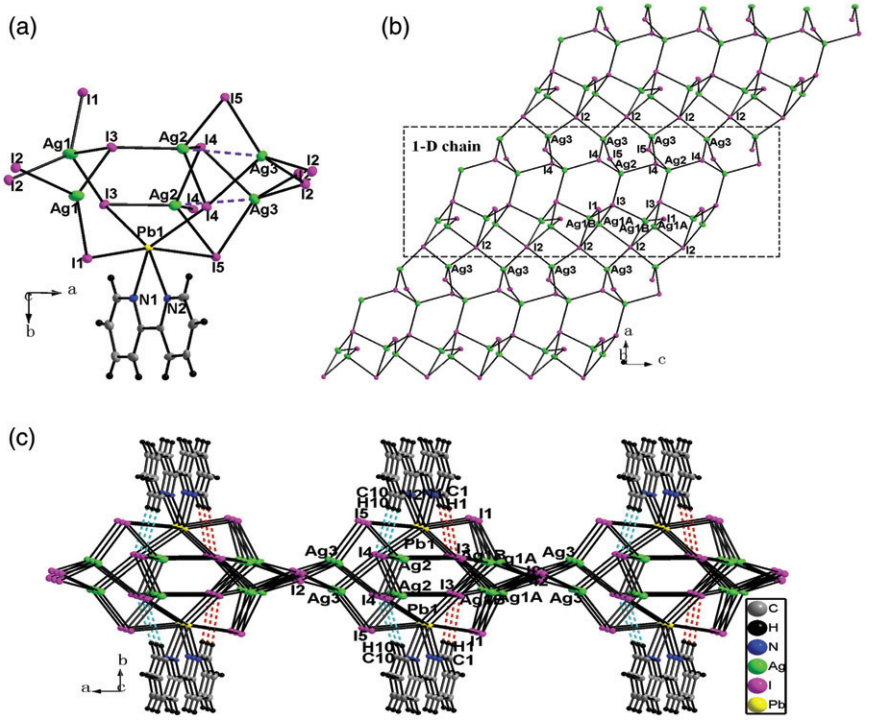

Figure 2. (a) Ag_6I_{14} building block. (b) View of $[Ag_3I_5]_n^{2n-}$ 2-D layer. (c) View of $[Pb(bipy)Ag_3I_5]_n$ (**2**) 2-D layer along the *c*-axis (red and blue dashed lines represent C–H···I hydrogen bonds).

chain *via* I(2) and I(5) and in the *a*-direction, by μ_4-I(2), forming a 2-D layer (figure 2b). In the *b*-direction, μ_2-I(1), μ_3-I(5), and μ_4-I(3) link with $[Pb(2,2'\text{-bipy})]^{2+}$ adopting six-coordinate distorted octahedral geometries with Pb–I distances of 3.080(24) and 3.507(18) Å. The bond length of Pb(1)–I(3) [3.507(18) Å] is relatively weak compared with commonly observed Pb(II)–I covalent bonds [22, 23]. C(1)–H(1)···I(3)#1 [3.845(16) Å, 149.65°] and C(10)–H(10)···I(4) [3.778(16) Å, 144.96°] hydrogen-bond interactions (table 5) could also be observed between bipy rings and $(Ag_3I_5)_n^{2n-}$ on the same 2-D layer, contributing to crystal stabilization (figure 2a and c).

Both complexes are neutral frameworks and can be compared with other kinds of complexes including negative Ag/I frameworks, in which organic cations or metal–organic complex cations are countercations [7–12]. Generally, a neutral framework will exhibit much better thermal stability.

3.2. *Absorption spectrum and linear absorption optical studies*

The purities of the compounds have been proved by XRD (Supplementary material), in which the experimental value is in good agreement with the theoretical simulation. So the measured properties reflect the behavior of bulk solid. The room-temperature UV-Vis absorption spectra of **1** and **2** can be seen in "Supplementary material." Absorptions at shorter wavelengths (220, 259, 250 nm) can be attributed to the π–π^* transfer of phen and bipy, and peaks at longer wavelengths (466 and 386 nm) stem from

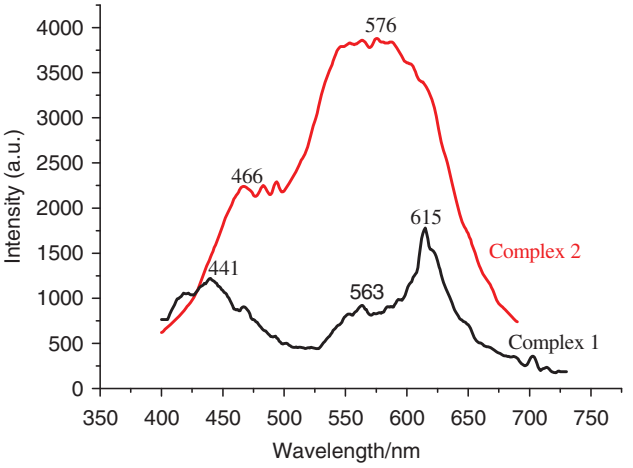

Figure 3. Solid-state emission spectra of **1** and **2** at room temperature.

an exciton state associated with the inorganic heterometallic iodoargentate moieties [24]. The optical absorption spectra of **1** and **2** have been measured by diffuse-reflectance experiments. The absorption edges of the compounds are 2.29 and 2.77 eV, showing that the complexes are semiconductors (Supplementary material; the values of E_g were obtained with the use of a straightforward extrapolation method [25, 26]). They exhibit 0.52 and 0.04 eV red shifts of the absorption edges compared with the measured value of 2.81 eV for bulk β-AgI. For **1**, compared with the band gap of bulk BiI_3 (1.73 eV), a blue shift of 0.56 eV has occurred; for **2**, a 0.47 eV blue shift compared with bulk PbI_2 (2.30 eV) was observed.

3.3. *Fluorescence properties*

Luminescence spectra excited at 250 nm for solid **1** and **2** are given in figure 3. Complex **1** exhibits much weaker luminescence at 441, 563 and 615 nm than **2** and **2** shows emission at 466 and 576 nm. For **1**, the shoulder emissions at 441 nm should be assigned to the ligand-to-metal charge transfer (LMCT) of phen to Ag/Bi, and 563 and 615 nm emissions should be explained as LMCT of I to Ag/Bi centers. For **2**, the emission at 466 nm could be attributed to the LMCT of phen to Pb and emission at 576 nm, which is very similar to that of $[PbAg_2(PPh_3)_2I_4]_n \cdot [PbI_2(DMF)_2]_n$ [16], can be assigned to the transition in the inorganic $[Ag_3I_5Pb]_n$ framework [27]. Similar assignments have been suggested and verified by molecular orbital calculation results for some related iodoargentates [7].

3.4. *Thermal properties*

Thermogravimetric analysis of **1** (TGA, Supplementary material) shows weight loss (15.4%) at 275–349°C, in good agreement with the calculated value of 15.2% for removal of one phenanthroline bonding with Ag^+. When the temperature is higher than 349°C, another phenanthroline bonding with Bi^{3+} begins to decompose. At the same

time, I^- also begin to decompose and the structure collapses. Residual weight (Bi^{3+} and Ag^+) is 26.5% (Calcd 26.6%). TGA trace of **2** (Supplementary material) shows a mass loss of 11.9% between 198°C and 319°C, attributed to loss of 2,2′-bipyridine (Calcd 11.8%). When the temperature is higher than 475°C, I^- anions begin to decompose and the structure collapses. The residual weight (Pb^{2+} and Ag^+) is 40.0% at 792°C, which agrees with the calculated value of 40.2%.

4. Conclusion

Introduction of Bi^{3+} and Pb^{2+} into the Ag/I system leads to two new heterometallic iodoargentates with 2-D layer arrangements $[Bi(phen)I_4Ag(phen)]_n$ (**1**) and $[Pb(bipy)Ag_3I_5]_n$ (**2**). They are semiconductors judging from their optical band gaps and exhibit fluorescence. Incorporation of other metals into the Ag/I system, such as Mn^{2+}, Co^{2+}, and Ni^{2+} or luminescent Ln^{3+} (Ln = rare earth metal) are ongoing.

Supplementary material

CCDC-731693 (for **1**) and 708 215 (for **2**) contain the supplementary crystallographic data for this article; these data can be obtained free of charge at www.ccdc.cam.ac.uk/conts/retrieving.html (or from the Cambridge Crystallographic Data Centre (CCDC), 12 Union Road, Cambridge CB2 1EZ, UK; Fax: +44(0)1223-336-033; E-mail: deposit@ccdc.cam.ac.uk).

Acknowledgments

We acknowledge support of this research by National Natural Science Foundation of China (No. 20901017), Specialized Research Fund for the Doctoral Program of Higher Education of China (20093514120003) and Scientific Research Foundation of Distinguished Young Scholars of Fujian Higher Education Institutions (JA10007).

References

[1] G. Xu, G.C. Guo, M.S. Wang, Z.J. Zhang, W.T. Chen, J.S. Huang. *Angew. Chem. Int. Ed.*, **46**, 3249 (2007).
[2] W. Bi, N. Louvain, N. Mercier, J. Luc, I. Rau, F. Kajzar, B. Sahraoui. *Adv. Mater.*, **20**, 1013 (2008).
[3] N. Mercier, N. Louvain, W. Bi. *CrystEngComm*, **11**, 720 (2009).
[4] L.M. Wu, X.T. Wu, L. Chen. *Coord. Chem. Rev.*, **253**, 2787 (2009).
[5] A.M. Goforth, M.A. Tershansy, M.D. Smith, L. Peterson Jr, J.G. Kelley, W.J.I. DeBenedetti, H.C. zur Loye. *J. Am. Chem. Soc.*, **133**, 603 (2011).
[6] A. Kojima, K. Teshima, Y. Shirai, T. Miyasaka. *J. Am. Chem. Soc.*, **131**, 6050 (2009).
[7] H.H. Li, Z.R. Chen, J.Q. Li, C.C. Huang, Y.F. Zhang, G.X. Jia. *Cryst. Growth Des.*, **6**, 1813 (2006).
[8] H.H. Li, Z.R. Chen, J.Q. Li, C.C. Huang, Y.F. Zhang, G.X. Jia. *Eur. J. Inorg. Chem.*, 2447 (2006).
[9] W.Z. Chen, F.H. Liu. *J. Organomet. Chem.*, **673**, 5 (2003).

[10] G.C. Xiao. *J. Cluster Sci*., **17**, 457 (2006).
[11] G.A. Bowmaker, Effendy, B.W. Skelton, N. Somers, A.H. White. *Inorg. Chim. Acta*, **358**, 4307 (2005).
[12] Y.J. Zhao, W.P. Su, R. Cao, M.C. Hong. *Acta Crystallogr., Sect. C*, **55**, 9900122 (1999).
[13] S. Mishra, E. Jeanneau, G. Ledoux, S. Daniele. *Dalton Trans*., 4954 (2009).
[14] S. Mishra, E. Jeanneau, S. Daniele, G. Ledoux. *Dalton Trans*., 6296 (2008).
[15] Y.S. Jiang, H.G. Yao, S.H. Ji, M. Ji, Y.L. An. *Inorg. Chem*., **47**, 3922 (2008).
[16] L.Q. Fan, L.M. Wu, L. Chen. *Inorg. Chem*., **45**, 3149 (2006).
[17] W.X. Chai, L.M. Wu, J.Q. Li, L. Chen. *Inorg. Chem*., **46**, 1042 (2007).
[18] H.H. Li, Z.R. Chen, L.G. Sun, Z.X. Lian, X.B. Chen, J.B. Li, J.Q. Li. *Cryst. Growth Des*., **10**, 1068 (2010).
[19] G.M. Sheldrick. *SHELXL-97*, *Program for X-ray Crystal Structure Refinement,* University of Göttingen, Germany (1997).
[20] Y. Chen, Z. Yang, X.Y. Wu, C.Y. Ni, Z.G. Ren, H.F. Wang, J.P. Lang. *Phys. Chem. Chem. Phys*., **13**, 5659 (2011).
[21] K. Nomiya, S. Takahashi, R. Noguchi. *Dalton Trans*., 2091 (2000).
[22] J.B. Liu, H.H. Li, Z.R. Chen, L.Q. Guo, C.C. Huang, J.Q. Li. *CrystEngComm*, **11**, 545 (2009).
[23] Z. Tang, A.P. Litvinchuk, H.G. Lee, A.M. Guloy. *Inorg. Chem*., **47**, 9333 (2008).
[24] H.H. Li, J.X. Wu, H.J. Dong, Y.L. Wu, Z.R. Chen. *J. Mol. Struct*., **987**, 180 (2011).
[25] W.W. Wendlandt, H.G. Hecht. *Reflectance Spectroscopy*, Interscience, New York, NY (1966).
[26] O. Schevciw, W.B. White. *Mater. Res. Bull*., **18**, 1059 (1983).
[27] G.H. Zhu, Y.J. Xu, Z. Yu, Q.J. Wu, H.K. Fun, X.Z. You. *Polyhedron*, **18**, 3491 (1999).